224 (2023) 211619

Contents lists available at ScienceDirect

Geoenergy Science and Engineering

journal homepage: www.sciencedirect.com/journal/geoenergy-science-and-engineering

Assessment of a surface-active ionic liquid formulation for EOR applications: Experimental and simulation studies

Nestor Tafur [a,**], Alba Somoza [a], Alberto P. Muñuzuri [b], Borja Rodríguez-Cabo [c], Izaskun Barrio [c], Asier Panadero [d], M. Flor García-Mayoral [d], Ana Soto [a,*]

[a] CRETUS, Department of Chemical Engineering, Universidade de Santiago de Compostela, E-15782, Santiago de Compostela, Spain
[b] Group of Nonlinear Physics, Dept. of Physics, Universidade de Santiago de Compostela, E-15782, Santiago de Compostela, Spain
[c] CEPSA-Química, Research Center, E-28805, Madrid, Spain
[d] CEPSA, Research Center, E-28805, Madrid, Spain

ARTICLE INFO

Keywords:
Blend
Microemulsion
Flooding
History match

ABSTRACT

This study aims to assess a surfactant blend for enhanced oil recovery from carbonate rocks. Due to the abundance of these reservoirs, their profitable exploitation would ensure our petrochemical needs are met, and maintain current quality of life. The objective of this work is to increase the technology readiness level of our previous proposal based on the use of a blend of pure sodium dodecylbenzene sulfonate and the surface-active ionic liquid cocosalkylpentaethoximethyl ammonium methylsulfate. To that aim, the method was adapted for its application with a commercially available petrochemical surfactant (RECOLAS103, a mixture of lineal alkyl benzene sulfonates), and reservoir simulations were carried out to evaluate its effectiveness. Phase behavior, stability, dynamic interfacial tension, adsorption and core flooding were the experimental tests carried out. An optimized formulation consisting of 1 wt% of blend (40 wt% RECOLAS103) in synthetic sea water was found stable and able to reduce water-oil interfacial tension down to 0.02 mN/m. The dynamic blend adsorption in carbonate rocks was found to be 0.60 mg/grock, a promising value for the application. Core flooding tests were conducted at 25 and 120 °C and additional oil recoveries achieved ranged from 10.2 to 12.7% of the original oil in place, the lowest production obtained at the highest temperature. This work offers an advance in the application of surfactants for EOR in carbonate reservoirs, since it improves previous proposals that show stability or high adsorption problems. Moreover, a chemical injection optimization was also carried out by simulation with the CMG-STARS software. Results point to the possibility of reaching higher oil recoveries than those obtained experimentally if the extraction method is optimized.

1. Introduction

In the current world energy scenario, it is expected that oil fields at developing and mature stages optimize their production. During the transition to the use of renewable energies, a more efficient extraction of the recoverable oil reserves must be achieved with the implementation of Enhanced Oil Recovery (EOR) techniques. These methods are mainly focused on the reduction of the residual oil saturation after water flooding by increasing the capillary number (N_C), which represents the ratio of viscous to capillary forces. This dimensionless number ranges normally from the order of 10^{-7} to 10^{-6} for water flooding. To reduce the water flooding residual oil saturation, N_C needs to be increased higher than the critical capillary number (normally around 10^{-5} to 10^{-4}) to mobilize the residual oil (Ghadami et al., 2015; Green and Willhite, 2018; Hakiki et al., 2015; Sheng, 2013, 2011). To achieve such a high N_C, low or ultralow values (around 10^{-3} to 10^{-2} mN/m) of water-oil interfacial tension (IFT) are required. These values can be obtained by injecting certain surfactants at specific conditions (Abbaszadeh and Ren, 2013; Kamal et al., 2017; Spildo et al., 2012), promoting the formation of optimal microemulsions within the reservoir. Surfactant injection reduces capillary pressure within the porous medium and alters the original relative permeability curves, reducing the residual oil saturation.

It is currently known that anionic surfactants show much greater

* Corresponding author.
** Corresponding author.
E-mail addresses: nestor.tafur@usc.es (N. Tafur), ana.soto@usc.es (A. Soto).

https://doi.org/10.1016/j.geoen.2023.211619
Received 16 September 2022; Received in revised form 6 February 2023; Accepted 24 February 2023
Available online 5 March 2023

efficiency in reducing IFT compared to cationic and non-ionic surfactants. However, they work better in sandstone reservoirs, whose surface rock has a negative electrical charge, than in carbonate reservoirs that are positively charged. In the latter case, a greater electrostatic adsorption of the anionic surfactant during injection drastically reduces the efficiency of the EOR project (Barati-Harooni et al., 2016; Ma et al., 2013; Scamehorn et al., 1982; Sheng, 2011; Wang et al., 2015). Several recent works propose the use of binary mixtures of anionic, cationic and nonionic surfactants for EOR applications, aiming to improve certain properties (i.e., IFT or surfactant adsorption) in comparison to the use of the single surfactants (Feng et al., 2018; Kurnia et al., 2020; Li et al., 2017, 2020; Pal et al., 2019).

Recently, the use of certain ionic liquids (salts with melting or glass transition temperatures below 100 °C) with surface-active properties has also been investigated. These salts, at very low concentrations in water formulations act as surfactants (Cooper et al., 2004; Hanke and Lynden-Bell, 2003) and are being studied to improve current EOR methods. A summary of these works was presented by Somoza et al. (2022a). Although those surface-active ionic liquids (SAILs) are capable of lowering IFT, they are rarely able to achieve ultra-low values by themselves (Fernández-Stefanuto et al., 2018). However, mixtures of SAILs and traditional surfactants have been shown able to achieve low IFT values ($<10^{-1}$ mN/m). Core flooding tests, in sandstone rocks or sand packs, have been used to validate the interest of these blends for EOR in these kinds of rocks (Jia et al., 2017; Nandwani et al., 2018).

The percentage of the world's oil found in carbonate reservoirs is commonly estimated at around 50–60% (Akbar et al., 1995; Burchette, 2012), so one of the priorities of the oil industry is to maximize the oil recovery from these rocks. The challenging conditions of carbonate reservoirs have led to a limited number of studies with surfactants in this kind of rocks. The SAIL [C_{18}mim]Cl was tested by Manshad et al. (2017) and Zabihi et al., (2019) leading to an additional oil recovery (AOR) of 13 and 16.5% OOIP, respectively. However, a high adsorption took place (according to the presented Freundlich isotherm) in the first study, and no information about this parameter was given in the second case. Nandwani et al. (2019b) proposed the use of a blend constituted by Tergitol 15-S-9 and the SAIL [P_{44416}]Br, achieving an AOR of 16.7% OOIP. The same authors exchanged the phosphonium SAIL for [C_{16}mim]Br to work at high salt concentration (31 wt%) and achieved an AOR of 20.9 %OOIP (Nandwani et al., 2019). However, those studies did not consider the presence of divalent ions, and were performed with an unconsolidated calcite powder packed bed. Montes et al. (2018) achieved an AOR of 32 %OOIP with a blend of alkyl benzene sulfonate + alkyl ethoxy carboxylate (40/60). However, the high adsorption of the blend (3.51 mg/g rock) would likely limit its application. Thus, the design of a formulation based on surfactants, or SAILs, able to satisfactorily extract oil from carbonate reservoirs is still a research goal.

In our previous report (Somoza et al., 2022b), a blend constituted of the anionic surfactant sodium dodecyl benzene sulfonate (SDBS) and the SAIL cocosalkylpentaethoximethyl ammonium methylsulfate was shown promising for EOR in carbonate reservoirs. As a continuation of that previous work, in this study the pure commercial SDBS was exchanged for a lineal alkyl benzene sulfonate surfactant (RECOLAS103) developed by CEPSA. The novelty and main contribution of this paper is, therefore, an approach to the real application of the proposed blend in EOR projects. To that aim, new laboratory tests were carried out to optimize the formulation with this petrochemical surfactant according to IFT and adsorption parameters. Further, numerical simulation studies were carried out to evaluate key chemical displacement parameters and to optimize the field chemical injection protocol, using the commercial reservoir simulator CMG-STARS (CMG, 2016).

2. Materials and methods

2.1. Experimental

2.1.1. Materials

The cationic SAIL cocosalkylpentaethoximethyl ammonium methylsulfate, commercially named IoLiLyte C1EG (hereinafter called "C1EG"), was purchased with purity ≥95 wt% from Iolitec. The surfactant RECOLAS103 is a sodium alkyl benzene sulfonate provided by CEPSA with a concentration of 20 wt%, with alkyl chain lengths C_{10}–C_{13}. The nonionic polymers polyacrylamide FloPAM FA 920 SH (6.5–8.5 × 10^6 Da) and FloPAM FA 920 VHM (≥8.5 × 10^6 Da) were kindly provided by SNF Floerger.

Two brines, synthetic formation water (SFW) and synthetic sea water (SSW), were used for initial water saturation and water flooding processes. The composition and densities of the SFW and the SSW are shown in Table 1.

Potassium iodide (KI), used as tracer for dynamic adsorption tests, was purchased from Sigma-Aldrich with purity >99 wt%. No further purification was done for the received chemical reagents. Distilled water was used to prepare C1EG and RECOLAS103 stock solutions, as well as the SFW and SSW.

N-octane was purchased from Sigma-Aldrich with a purity >99 wt%. Two dead crude oils were used in this work, both provided by CEPSA. Their main characteristics are presented in Table 2.

Indiana Limestone carbonate rocks were used for dynamic adsorption and core flooding experiments at room conditions (plug of 8–20 mD permeability and dimensions of 75.3 mm length and 38.2 mm diameter) and 120 °C (plug of 2–5 mD permeability and dimensions of 111.1 mm length and 37.7 mm diameter).

2.1.2. Methods

To avoid individual interactions of C1EG and RECOLAS103 with divalent salts before mixing, stock solutions were prepared for each component in distilled water at 8 wt% concentration of active matter. All of the solutions were prepared by weight using a Mettler Toledo XPE205 analytical balance. Weighing uncertainty was 0.0001 g.

2.1.2.1. Blend scans. Phase behavior of the surfactant blend was evaluated through mixing ratio scan tests using the encased-glass-pipette methodology (Barnes et al., 2008; Puerto et al., 2012). The aqueous and oily phases were introduced into tip sealed borosilicate glass pipettes, then heat-sealed at the top, and mixed slowly for 24 h at ambient temperature with the use of a rotary mixer. Finally, pipettes were placed in 10 mL test tubes containing silicon oil, and set to equilibrate in an OVAN bath dry block (model BD200-RE) at the required temperature until no change in interfacial position was observed.

The water-oil ratio in the pipettes was around 1:1, with ~1 mL of *n*-octane as the oil phase and ~1 mL of aqueous phase with 4 wt% surfactant concentration. The blend scan was performed at different RECOLAS103/C1EG mass ratios, from 100/0 to 0/100 (weight). The salinity of the aqueous phase was 4.97 wt% TDS (SSW). Phase behavior was evaluated at 25 °C, 50 °C and 75 °C. Phase volumes were measured to calculate solubilization parameters defined as either volume of oil (V_o)

Table 1
Compositions, salt purities and densities for synthetic formation water (SFW) and synthetic sea water (SSW).

Salt	Purity (wt%)/Commercial	SFW (g/L)	SSW (g/L)
Na_2SO_4	>99%/Sigma-Aldrich	0.4	4.84
$CaCl_2{\cdot}2H_2O$	>99%/Sigma-Aldrich	61.1	1.89
$MgCl_2{\cdot}6H_2O$	>99%/Sigma-Aldrich	13.1	15.06
NaCl	>99%/Panreac	153.5	27.94
$NaHCO_3$	>99%/Scharlau	0.5	0
TDS (g/L)		228.6	49.73
Density at 25 °C (g/mL)		1.100	1.028

Table 2
Main properties of used crude oils.

Property	Crude oil A	Crude oil B
Density at 25°C (g/mL)	0.853	0.836
°API	34.1	37.3
Viscosity at 25°C (mPa·s)	15.3	5.38
Saturates (wt%)	61	71
Aromatics (wt%)	33	28
Resins (wt%)	4.6	1
Asphaltenes (wt%)	1.4	<1

or water (V_w) solubilized per volume of surfactant (V_s) in the micro-emulsion phase (Montes et al., 2018; Puerto et al., 2012; Rodriguez-Escontrela et al., 2017; Somoza et al., 2022b). The optimal solubilization parameters (V_i/V_s*, when $V_o/V_s = V_w/V_s$) were used to estimate the IFT between the aqueous and oleic phases by using the Huh's correlation (Huh, 1979):

$$IFT_{Huh} = \frac{C}{\left(V_i/V_S^*\right)^2} \quad \text{(Eq. 1)}$$

where C is an empirical constant ranging between 0.1 and 0.35 mN/m. It was fixed at 0.3 in the present work.

The presence of liquid crystals in the systems was evaluated through the search of birefringence under polarized light.

2.1.2.2. Compatibility tests. The stability of the blend in the absence of oil was evaluated at different mixing ratios to determine the possible separation of the components, leading to their non-uniform distribution in the reservoir during injection, as well as the appearance of precipitates. The evaluation was carried out visually based on the translucence of the solution. To this end, formulations at several blend ratios were prepared (1 wt% blend concentration) in SSW (4.97 wt% TDS) at room temperature (Kurnia et al., 2020; Somoza et al., 2022a,b).

2.1.2.3. Dynamic interfacial tension. IFT measurements between crude oil A and the aqueous formulations (1 wt% blend concentration) were performed at 25 °C with the use of a Krüss spinning drop tensiometer (model SITE100) as in our previous reports (Somoza et al., 2022a,b). The main purpose of this study was the selection, among the promising blends found with the phase behavior studies, of the mixture leading to the lowest IFT. During the measurements, an oil drop of 4 μL was injected into the capillary tube of the equipment previously filled with the aqueous formulation. The rotation speed was set in order to obtain a drop length at least four times larger than its diameter. An Anton Paar density meter (model DMA 5000 M) was used to measure the densities of the phases. The relative standard uncertainty of equilibrium IFT was estimated to be 10%.

2.1.2.4. Dynamic adsorption. Single-phase dynamic adsorption tests were carried out in a Hassler core holder equipment (model H00-021-0) at room temperature. A carbonate rock core was used for these tests with a confining pressure set to 700 psi. After vacuuming the core for 24 h, it was saturated with SSW at an injection rate of 0.05 mL/min, also for 24 h. The absolute permeability (K_a) was estimated by Darcy's Law at different injection rates with their stabilized differential pressures. After the estimation of pore volume and porosity, potassium iodide (KI) was injected as the tracer at 0.1 mL/min, and effluent samples were taken roughly every 1 mL until reaching the initial KI concentration (C_0). Next, the core was cleaned by injecting SSW until no traces of KI were detected. The optimized RECOLAS103/C1EG formulation was then injected with the same protocol and conditions. An HP UV/Vis-spectrophotometer (model Presario SR1000) was used to estimate the concentrations of tracer and blend in effluents during the test. The blend adsorption was estimated based on the delay in the surfactant front in comparison with the tracer front by using the following equation (Montes et al., 2018; Sharma et al., 2016; Somoza et al., 2022b):

$$\tau = \frac{\left(PV_{blend,50\%} - PV_{tracer,50\%}\right) \times PV \times [C_0]_{blend}}{mass_{rock}} \quad \text{(Eq. 2)}$$

where τ is the blend adsorption in mg/g, $PV_{blend,50\%}$ and $PV_{tracer,50\%}$ are the pore volume in which blend or tracer concentration reached 50% of initial concentration, PV is the pore volume in mL, $[C_0]_{blend}$ is initial blend concentration in mg/mL, and $mass_{rock}$ is the dry core weight in grams. Adsorption uncertainty was estimated to be 0.02 mg/g rock.

2.1.2.5. Polymer solution evaluation. Although the optimum selection of a polymer to efficiently sweep a 15.3 mPa s crude oil through low permeability carbonate cores (25 mD or less) is outside the scope of this study, a preliminary evaluation of two polymers was performed to define the type and the polymer concentration to use in this work. Two nonionic polymers (FloPAM FA 920 SH and FloPAM FA 920 VHM) were analyzed. Polymer solutions were prepared by weight adding polymer powder to SSW. 5000 ppm stock solution was prepared by stirring the solution at 80 rpm with a magnetic stirrer for 3 h, ensuring the absence of large slugs or "fish-eyes", then allowing the solution to settle overnight. More diluted polymer solutions were prepared by mixing the stock solutions with SSW gently stirring overnight (14 h). The whole process was carried out at room temperature and following the recommended practices for evaluation of polymers used in enhanced oil recovery operations (American Petroleum Institute- Production Department, 1990).

Apparent viscosities (η) for both polymer solutions were determined as a function of polymer concentration and shear rate at 25 °C, using an Anton Paar rheometer (model MCR 102), to choose the suitable polymer and concentration. The relative standard uncertainty of viscosity was 3%. Injectivity tests of the polymer solutions were carried out in fresh carbonate cores saturated with SSW at room conditions to define the polymer formulation to be used in flooding tests.

2.1.2.6. Core flooding tests. In general, for each displacement test, the cores were initially vacuumed and then saturated with brine using the core holder equipment. Absolute permeabilities (K_a) were estimated using Darcy's law, while pore volumes (PV) and porosities ($Ø$) were calculated using wet and dry core weights and the water density. Water was drained by injecting dead crude oil to reach the initial water saturation (S_{wi}) and the cores were left to equilibrate or for ageing. The total expelled water was used to calculate the original oil in place (OOIP). Fresh oil was injected, and maximum oil relative permeability (K_{romax}) was estimated. Then, the cores were water flooded with SSW and volumes of produced oil, produced water, injected water and differential pressures were recorded. The residual oil saturation for water flooding (S_{orw}) and the oil recovery were estimated from material balance. The end-point water relative permeability (K_{rwmax}) was estimated at the end of the water flooding process. Surfactant flooding was conducted by injecting optimized blend formulation (1 wt% concentration), and residual oil saturation after chemical flooding (S_{or2}) and oil recovery were calculated.

Three core flooding experiments were carried out to determine the efficiency of the blend under different conditions. The CF-1 test was an initial study carried out at room temperature with the sole purpose of evaluating the EOR capacity of the proposed blend, and the comparison of the results with previous studies (Somoza et al. 2022b). This test was not considered in posterior simulation studies. CF-2 was conducted at 120 °C to evaluate the effect of the temperature on the oil recovery. The third test (CF-3) was carried out using a more realistic protocol of injection, flooding a slug of the blend followed by a polymer flood at injection rate around 1 ft/D. In this test, effluent samples were collected for salinity analysis with a Crison conductivity meter (model Basic 30). Finally, chase water was injected to estimate the residual resistance

factor (RRF) of the polymer using the following equation:

$$RRF = \frac{\Delta P_{Chase\ water\ flood}}{\Delta P_{Water\ flood}} \quad \text{(Eq. 3)}$$

where ΔP_{Water_flood} and $\Delta P_{Chase\_Water\_flood}$ are the stabilized differential pressures at the end of the water and the chase water flooding, respectively. A summary of the protocols for CF-1, CF-2 and CF-3 is presented in Table 3.

2.2. Simulation

Dynamic numerical simulations were performed using the compositional reservoir simulator CMG-STARS (CMG, 2016) with the main objective of confirming the surfactant blend parameters (IFT and adsorption measurements) during flooding, and also determining unknown parameters involved in the process.

2.2.1. Model system

The fluids flow along the core mainly in one direction during core flooding, with the radial flow being negligible (Kornilov et al., 2020; Kumar and Mandal, 2020). Thus, for the simulation of CF-2 and CF-3 tests, the cores were represented using 3D grids in Cartesian coordinates (X, Y, Z), with 11 grid blocks in the flow direction X (11 × 1 × 1). Fig. S1 and S.2 in the Supplementary Information (SI) show the grid sensitivity study carried out to determine the independence of the results from the grid resolution. Inlet and outlet flow points were set at each end of the grid. The grids were built to represent the core dimensions (length and cross-sectional area) and introduce rock characteristics (porosity and absolute permeability) and fluid properties at the corresponding test temperature (density and viscosity of water and oil phases). The flow of the fluids through the porous medium was modeled by the incorporation of relative permeability curves, which were built using Corey's correlations, and the end-points from the core flooding tests (S_{wi}, S_{orw}, K_{romax}, *and* K_{rwmax}). Data were initially introduced into the models with no changes and without considering any error range in their measurements. This original set of relative permeability curves (Set 1) was generated for each experiment (CF-2 and CF-3) to simulate the water flooding process.

Regarding surfactant flooding, experimental IFT measurements and adsorption were also set in the models. CMG-STARS models the surfactant effects by using sets of relative permeabilities curves, which are a function of the capillary number *Nc* (Abbaszadeh and Ren, 2013; CMG, 2016; Van Quy and Labrid, 1983). Since the incorporation of surfactant decreases the IFT to ultra-low values it can theoretically straighten the relative permeability curves (Bardon and Longeron, 1980; Harbert, 1983; Ronde, 1992), CMG-STARS was used to generate this second set of curves (Set 2). In the simulation, both sets were used for surfactant flooding: Set 1 obtained through water flooding conditions (at normal interfacial tension) and Set 2 for completely miscible flooding (ideal straight lines for ultra-low interfacial tension). The interpolation between these two sets allowed the generation of multiple intermediate relative permeability curves for semi-miscible flooding by simulation, and also the reproduction of the experimental data.

To represent polymer flooding, the experimental data of the viscosity of SSW polymer formulations, as a function of polymer concentration and shear rates, were introduced into the model. Since polymer adsorption was not measured, an approximate value was used as a starting point, and it was considered one of the history matching parameters. Accessible Pore Volume (*APV*) was also initially estimated.

Table 3
Summary of core flooding protocols.

	CF-1	CF-2	CF-3
Test Temperature (°C)	25	120	25
Carbonate core aging	No	Yes	No
Initial saturation fluid	SSW	SFW	SFW
Crude oil	A	B	A
Water Flooding			
Injection rate (mL/min)	2.00	0.066 (~1 ft/D)	0.050 (~1 ft/D)
Injected fluid	SSW	SSW	SSW
Chemical Flooding			
Injection rate (mL/min)	2.00	0.066 (~1 ft/D)	0.050 (~1 ft/D)
Injected fluid	Blend	Blend	Blend slug + Polymer
Chase water Flooding			
Injection rate (mL/min)	–	–	0.050 (~1 ft/D)
Injected fluid	–	–	SSW

2.2.2. Model validation (history match)

Some parameters entered in the numerical models were not measured experimentally and were assumed as starting points for initial simulations, and others were estimated experimentally but not directly measured during the displacement tests. Therefore, those properties had to be validated and re-evaluated through model calibration (history matching study). After building the initial models for CF-2 and CF-3 flooding tests, history matching was carried out in two stages, the first one was done for the water flooding and the second one for the chemical flooding periods.

For the water flooding history matching, the parameters to validate were the endpoints related to the relative permeability curves, mainly K_{romax} and K_{rwmax}, since S_{wi} and S_{or} were experimentally determined. The absolute permeability as well as the Corey's exponents for water (N_w) and oil phases (N_o) were also considered. In the case of the surfactant injection, the re-evaluation parameters were the blend adsorption and the IFT, this latter through the intermediate sets of relative permeability curves for semi-miscible conditions. CMG-STARS uses the wetting phase and the non-wetting phase interpolation factors, DTRAPW and DTRAPN respectively, to modify the interpolated relative permeability curves. Both are functions of the capillary number (CMG, 2016; Hakiki et al., 2015; Kumar and Mandal, 2020). For polymer injection, the main tuning parameters considered were the adsorption and the accessible pore volume (APV). The residual resistance factor (RRF) was also considered in the study with a lower range of variations since it was approximated during the experimental test.

The objective variables (outcome to match) were the produced fluids (oil and water), the injection scheme, and the differential pressures. For the assisted history match processing, the CMG-CMOST-AI tool, which combines experimental design and artificial intelligence, was used. For the matching of each model (CF-2 and CF-3), the range of evaluation for the parameters was based on the uncertainty of their determination. The process finished once the global error between experimental and simulated results of the objective variables achieved a value lower than 10%. This study was performed through the CMG Bayesian engine.

2.2.3. Chemical slug optimization

The model with the lower deviation, obtained during the history matching process, was used as base case for the chemical injection. The effects of the formulation, slug size and injection rate, as well as the polymer viscosity when applicable, were used to determine the optimized injection protocol.

3. Results and discussion

3.1. Experimental section

3.1.1. Blend scans

The results of the blend scan at 25 °C can be seen in Fig. 1. Pure surfactants RECOLAS103 and C1EG presented Winsor I behavior at 25 °C and 5 wt% TDS of salinity. As in the case of the blend SDBS/C1EG (Somoza et al., 2022b), increasing the proportion of the sulfonate surfactant from 0 wt% to 50 wt%, the blend became more lipophilic and a

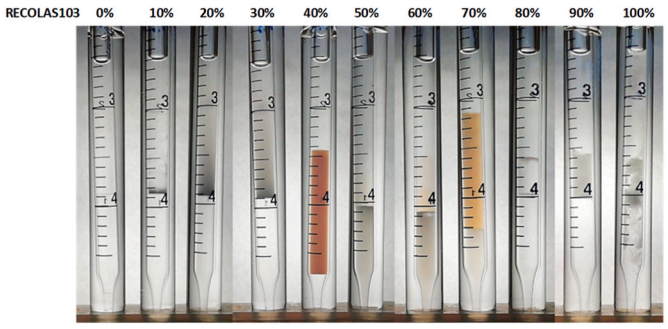

Fig. 1. Phase behavior evaluation for RECOLAS103/C1EG blend at 25 °C. Aqueous phase: 4 wt% blend in SSW; Oily phase: *n*-octane.

transition from Winsor I to Winsor III (at ~40 wt% RECOLAS103) and then to Winsor II (at equilibrated proportion of the components) was observed. The cationic C1EG and the anionic RECOLAS103, when blended, generated an optimal blend in Winsor III region (associated to ultra-low IFT and high oil recovery) caused by the electrostatic attraction between the oppositely charged surfactant head groups. The electrostatically neutral complex formed (a catanionic surfactant) exhibits many unique properties, due to the effective reduction of the area of surfactant head groups, and is less hydrophilic than the individual surfactants (Li et al., 2017; Puerto et al., 2012; Rodriguez-Escontrela et al., 2017; Somoza et al., 2022b). Increasing the proportion of RECOLAS103 from 50 to 100 wt% provoked the change of the microemulsion behavior from Winsor II to Winsor I, with a second Winsor III microemulsion at ~70 wt% RECOLAS103. This second blend leading to a Winsor III microemulsion was also found with SDBS (Somoza et al., 2022b) and was concluded to be less promising (higher adsorption, higher IFT and lower recovered oil) than the first one. For that reason, this work was focused on the applicability of the first blend for EOR applications.

As the behavior of the blend RECOLAS103/C1EG was very similar to SDBS/C1EG at 25 °C (Somoza et al., 2022b), similar behavior was also expected at higher temperatures. To confirm the hypothesis, blend scans were carried out at 50 °C and 75 °C (Fig. S3 and S4 in SI). A slightly different behavior was found at 50 °C, the blend presenting a three-phase region between 40 and 70 wt% RECOLAS103, with a significant reduction of the volume of water and oil solubilized. At 75 °C, as in the case of the SDBS/RECOLAS103 blend, a Winsor I-III-II-III-I transition was again found, with a Winsor III region corresponding to compositions ranging from 40 to 50 wt% RECOLAS103 and another Winsor III region at 70–80 wt% RECOLAS103. Fig. S5 (SI) shows the absence of liquid crystals for Winsor III microemulsions at 25 °C and 75 °C, although some liquid crystals were noticed at 50 °C between 40 and 60 wt% RECOLAS103.

In order to obtain the optimal solubilization parameters (V_i/V_s*), the solubilization parameters for oil (V_o/V_s) and water (V_w/V_s) were calculated for the optimal blend of interest (first one) at the three evaluated temperatures. Results are shown in Fig. 2. Increasing temperature from 25 °C to 75 °C reduced the V_i/V_s* value, which translates into reduced solubilization capacity of the formula. Table 4 shows the numerical values of the optimal solubilization parameters and optimal blend ratios, as well as the IFT estimated by Eq. (1). Slightly lower concentrations of sulfonate surfactant at the optimal blend ratio were found in this work

Table 4
Optimal blend ratios and solubilization parameters, and IFT_{Huh}, for the RECOLAS103/C1EG blend at 25 °C, 50 °C, and 75 °C.

	25 °C	50 °C	75 °C
Optimal blend ratio RECOLAS103/C1EG	42.3/57.7	39.1/60.9	38.7/61.3
V_i/V_s* [a]	14.37	6.83	5.46
IFT_{Huh} (mN/m)	1.45×10^{-3}	6.43×10^{-3}	1.01×10^{-2}

[a] First optimum (see the text).

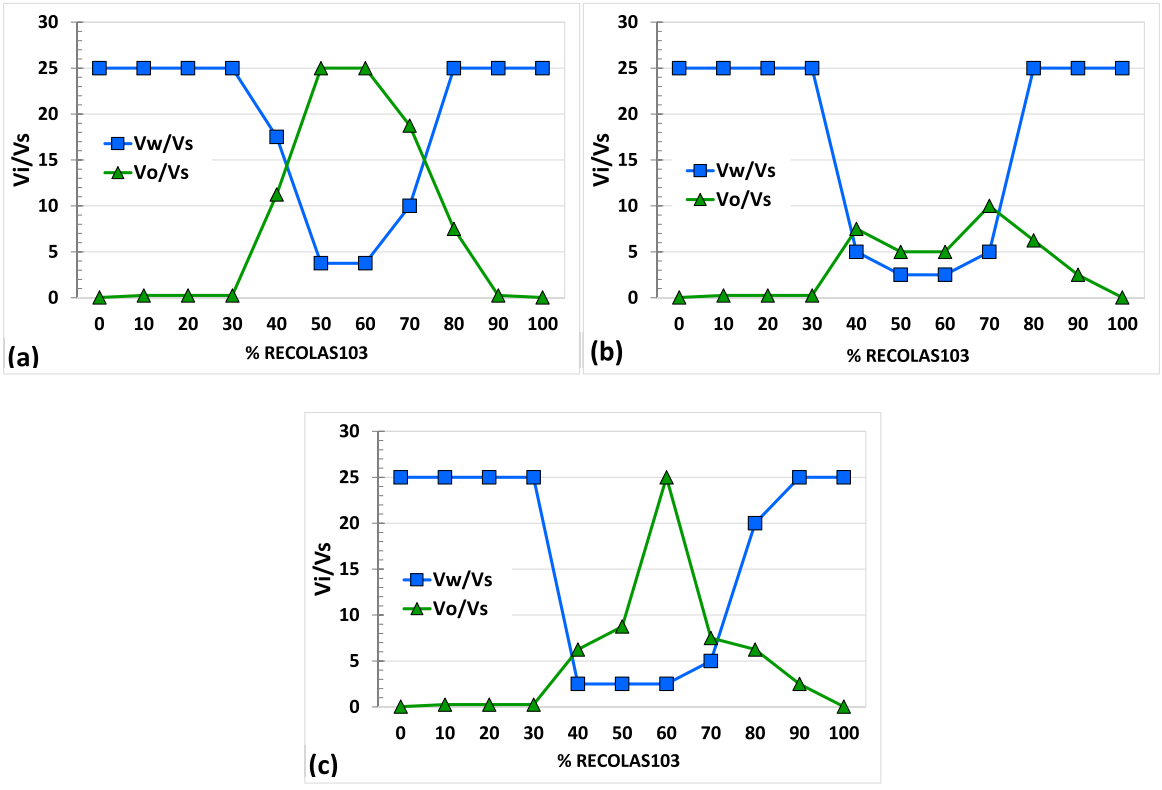

Fig. 2. Solubilization parameters (V_i/V_s) for RECOLAS103/C1EG blend at (a) 25 °C, (b) 50 °C, and (c) 75 °C. Aqueous phase: 4 wt% blend in SSW; Oily phase: *n*-octane.

with a petrochemical surfactant (used in practical applications) compared to our previous study with a pure commercial product (Somoza et al., 2022b). In addition, optimal solubilization parameters slightly decreased at 25 °C (14.4 with RECOLAS103 and 15.5 with SDBS) and increased at 50 and 75 °C (6.8 and 5.5 with RECOLAS103 and 3.7 and 3.3 with SDBS, at 50 and 75 °C, respectively). The differences being justified due to the mixture of chain lengths of the petrochemical surfactant.

3.1.2. Compatibility test

To ensure their compatibility, the stability of some formulations close to the optimal blend ratio was tested in SSW at 1 wt% blend concentration and room temperature. Mixtures with compositions in the blend ranging from 34 wt% to 44 wt% RECOLAS103 (step 2 wt%) were tested. As shown in Fig. 3, the blend presented stability in the evaluated ratios, keeping clear until the end of the test, after 4 weeks.

3.1.3. Dynamic interfacial tension (IFT)

The final selection of the best RECOLAS103/C1EG blend ratio was made based on IFT measurements. According to blend scan tests, Winsor III behavior (minimum IFT) was achieved at 38.7 wt% RECOLAS103 at 75 °C, and 42.3 wt% RECOLAS103 at 25 °C (see Table 4), so blend proportions ranging from 38 wt% to 45 wt% RECOLAS103 were selected. Fig. 4 shows the equilibrated IFT data at 25 °C as a function of blend ratios (for comparative purposes pure C1EG was also included, but RECOLAS103 precipitates in SSW). As shown, the RECOLAS103/C1EG blend reached the lowest IFT (2.1×10^{-2} mN/m) at a 40/60 ratio. In our previous work (Somoza et al., 2022b), the same optimal blend ratio was decided through IFT measurements, however, the IFT achieved was clearly lower (2.2×10^{-3} mN/m) than in the present case. As the surfactants behaved very similarly in previous tests, the reason is likely to be the type of crude. Crude oil components, especially resins and asphaltenes have significant influence on the IFT (Zhu and Lei, 2015). In the case of the work with SDBS (Somoza et al., 2022b), crude oil had a resin content of 11.6 wt%, 41.7 wt% of aromatics and 43.5 wt% of saturates. The crude oil used for IFT measurements in this work only has a 4.6 wt% resin content, and the content of aromatics is also lower (33 wt%), the saturate content clearly being higher (61 wt%). According to Zhu and Lei (2015), crude oil group components with the greatest effect on ITF reduction capacity are resins, followed by aromatic and finally saturates and wax content. So, the different composition of crude oils justifies the differences found in IFT measurements.

3.1.4. Adsorption

The adsorption obtained in our previous work for the blend SDBS/C1EG (Somoza et al., 2022b) was much lower in carbonate than in sandstone rocks, therefore the adsorption evaluation for the optimal blend RECOLAS103/C1EG was performed in a carbonate core at room temperature. Fig. 5 shows the relative concentration of the sampled effluents for the tracer (blue curve) and for the blend (green curve) as a function of the injected pore volume (PV) at room conditions. 50% of the initial tracer concentration (when $C/C_0 = 0.5$) was detected at 1.23 injected PV, while for the blend 2.13 PV was required. Using Eq. (2), the dynamic adsorption was estimated around 0.60 mg/g of rock. The electrostatic attraction between the surfactant head group and the rock surface is the most important mechanism of adsorption. The catanionic surfactant formed with the blend is an electrostatically neutral complex, which explains why the adsorption in carbonate material is low.

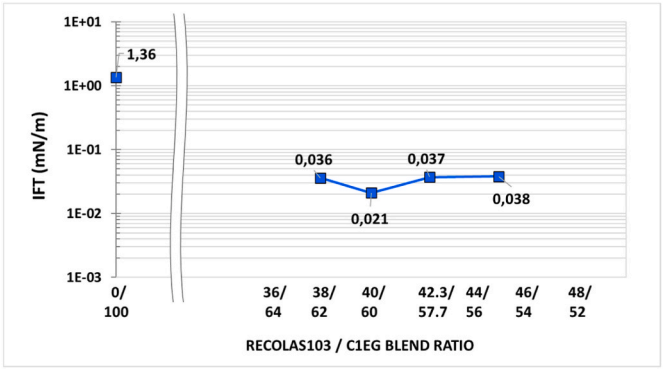

Fig. 4. Interfacial tension measurements at 25 °C and atmospheric pressure for RECOLAS103/C1EG formulations as a function of blend ratio. Aqueous phase: 1 wt% blend in SSW; Oily phase: crude oil.

3.1.5. Polymer solution evaluation

The apparent viscosity of different solutions, prepared in SSW, of two nonionic polymers (FloPAM FA 920 SH and FloPAM FA 920 VHM) was determined at 25 °C as a function of polymer concentration and shear rate (from 1 to 100 s^{-1}). Data are shown in SI (Fig. S6). Fig. 6 shows apparent viscosities at a shear rate of 10 s^{-1}. Due to the difficulty of getting an efficient displacement control with any of the polymers, injectivity tests for different polymer solutions were conducted in fresh carbonate cores. The results of those tests are presented in Fig. S7 and show the difficulty of matching polymer formulation and oil viscosities without plugging the core face due to the low permeability (17.7 mD) of the core. So, a compromise was struck: approaching the oil viscosity whilst also limiting polymer concentration to avoid plugging. The PAM 920 VHM polymer was selected to achieve an apparent viscosity $\eta = 6.3$ mPa s (at 10 s^{-1}) at a lower concentration (1500 ppm) than that required by the polymer PAM 920 SH (see Fig. 6).

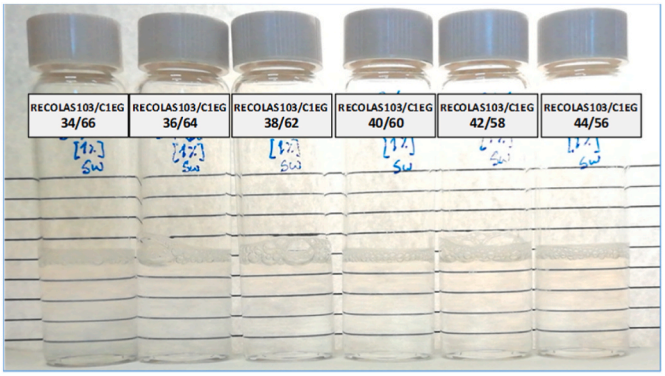

Fig. 3. Compatibility tests at room conditions for RECOLAS103/C1EG blends, at 1 wt% blend concentration and different surfactant ratios, in SSW and absence of oil phase.

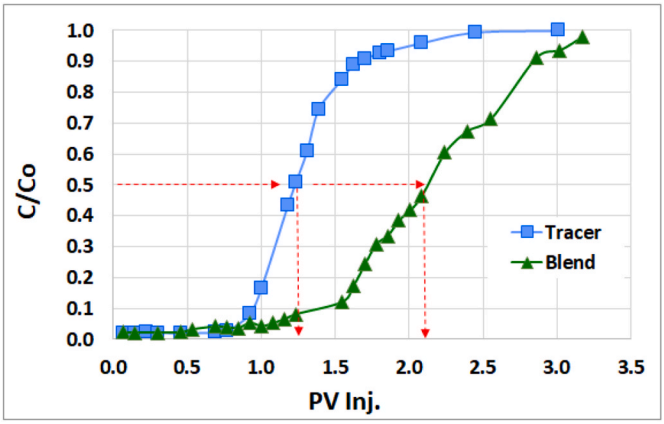

Fig. 5. Estimation of dynamic adsorption at room conditions for the optimal formulation (1 wt% blend - 40/60 RECOLAS103/C1EG-in SSW) in a carbonate core.

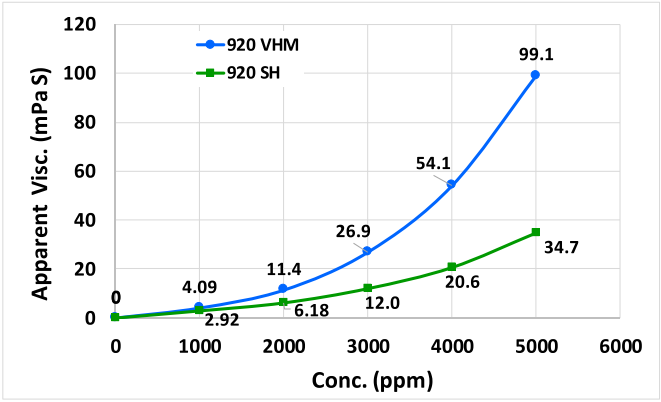

Fig. 6. Apparent viscosity, at 25 °C, atmospheric pressure and 10 s^{-1}shear rate, of FloPAM FA 920 VHM (blue) and FloPAM FA 920 SH (green) solutions prepared in SSW.

3.1.6. Core flooding tests

In the CF-1 test, the carbonate core (water-wet) was flooded with 4.2 PV of SSW at 2 mL/min (no oil production was observed by the end of the flood). Then, 4.34 PV of the optimized blend (1 wt% - 40 wt% RECOLAS103 - in SSW) were injected at 2 mL/min obtaining an AOR of 12.7% OOIP for this chemical flooding.

CF-2 was conducted at 120 °C and pore pressure of 91.4 psi with an intermediate-wet rock. The oil displacement was done by injecting SSW at 0.066 mL/min (~1 ft/D) until about 99% watercut and stable differential pressure across the core were observed, followed by 10.25 PV of the blend formulation at the same rate. The AOR was in this case 10.2% OOIP. Due to the very low permeability of the core (3.35 mD), no polymer was injected to avoid face plugging. The results of this test can be observed in Fig. 7.

For the CF-3 test, a water-wet carbonate rock was water flooded at 0.05 mL/min (~1 ft/D) until about 99% watercut and stable differential pressure across the core was observed. A blend slug of 0.56 PV was injected followed by 1.6 PV of polymer flooding, both at 0.05 mL/min. The AOR with this method was 11.7% OOIP. The chase water flooding was carried out to estimate the residual resistance factor (RRF) of the polymer, which was 1.4. Fig. 8 presents the oil recovery, differential pressures, residual oil saturation and salinity of the effluents for this core flooding test during the water (WF), blend (SF), and polymer (PF) floods. As shown, at 1.9 PV injected, the salinity of the effluent had already reached the SSW salinity used during the water flooding. Despite the polymer evaluation and the precautions taken, the rise of the injection pressure during polymer flooding shows slight but continuous face plugging. However, that did not influence the final efficiency of the blend greatly. The optimization of the polymer slug is outside the scope of this work.

Table 5 presents a summary of the three core flooding tests. The main mechanism associated to the improvement of oil recovery is IFT reduction. The blend of the cationic and anionic surfactants led to a catanionic species. Its aqueous formulation in contact with oil forms a Winsor III system associated with a very low IFT. This reduction is related to an increase in the capillary number, explaining the mobilization of trapped oil and the reduction of the residual oil saturation. The differences in the performance of the chemical flooding among the CF-2 with respect to the other two tests should be noted: the surfactant formulation lost efficiency at 120 °C when compared to CF-1 and CF-3 tests. Experimental conditions are different (core in CF-2 was aged), but the outcome is partially explained from results obtained in section 3.1.1, where a clearly low solubility of oil and water was achieved at the higher temperature. In the CF-2 test, the injection of more than 10 PV of blend was required to obtain an AOR of about 10% OOIP. Fig. 7 shows that 3 PV of blend formulation were required to start the oil displacement during surfactant flooding. When production ceased, a further 3.26 PV of blend formulation was injected to restart it.

3.2. Simulation

3.2.1. Model validation (history match)

In general, the numerical models of CF-2 and CF-3 tests were initialized for a first verification of the pore volume and OOIP. Afterwards, the models were run for the water flooding stage using initial values of the tuning parameters described in section 2.2.2. As indicated, the four end-points were obtained during the core flooding experiments. S_{wi} and S_{orw} (shown in Table 5), were directly taken from experimental data, while K_{romax} and K_{rwmax} were estimated by Darcy's law. A value of 2 was initially assigned to Corey's exponents, N_w and N_o, as a starting point for the iteration process. The simulated oil production, water production and differential pressures were compared with laboratory data from the CF-2 and CF-3 tests (Figs. 7 and 8). Results were not satisfactory, so to improve the match among them, parameters were tuned by a history matching process, to define the relative permeability curves that govern the water flooding (Set 1).

- ***CF-2 test***

For the CF-2 test, the simulation was done for better understanding and validate the mechanisms involved in the loss of productivity of blend flooding and in the differential pressure behavior. Table 6 shows the tuning parameters involved in this evaluation for water flooding, with the initial values for each parameter before history matching, their range of evaluation, as well as the defined values after the history matching.

Next, the simulation of blend injection was run with IFT and surfactant adsorption data obtained experimentally. Since the simulated

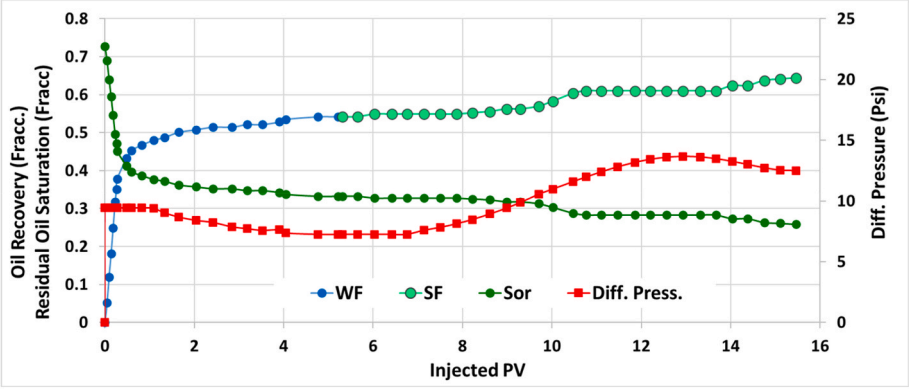

Fig. 7. Results of the displacement test CF-2 during the water (WF) and optimal blend (SF) floods at injection rate of 0.066 mL/min (~1 ft/D) and at 120 °C.

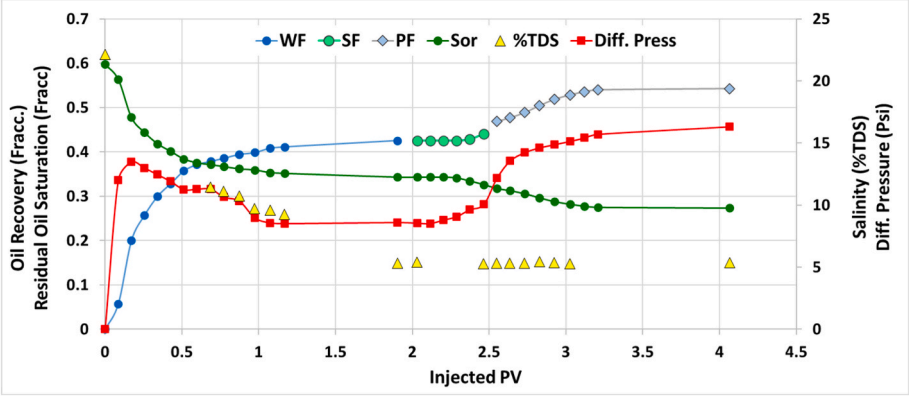

Fig. 8. Results of the displacement test CF-3 during the water (WF), optimal blend (SF), and polymer (PF) floods at injection rate of 0.05 mL/min (~1 ft/D) and at room conditions.

Table 5
Results of the core flooding experiments.

	CF-1	CF-2	CF-3
Porosity, ϕ (frac.)	0.147	0.177	0.134
Permeability, K_a (mD)	7.99	3.35	17.69
Pore Volume, PV (mL)	12.7	22.05	11.71
Oil Visc (mPa S) at test temp.	12	0.82	12
OOIP (mL)	8.4	16.03	7.0
Initial water saturation, S_{wi} (frac.)	0.338	0.273	0.402
Initial oil saturation, S_{oi} (frac.)	0.661	0.726	0.597
Water Flooding			
Injection rate, Qi (mL/min)	2.00	0.066	0.050
Injected SSW Volume (PV)	4.21	5.21	1.9
Oil Recovery (%OOIP)	59.5	54.2	42.5
Residual oil saturation, S_{orw} (frac.)	0.267	0.333	0.343
Chemical Flooding			
Injection rate (Q_i, mL/min)	2.00	0.066	0.050
Injected blend volume (PV)	4.34	10.25	0.56
Injected polymer volume (PV)	–	–	1.6
AOR (%OOIP)	12.7	10.2	11.7
Residual oil saturation, S_{or2} (frac.)	0.183	0.258	0.273

Table 6
Set of parameters for history matching of water flooding, test CF-2.

Parameter	Initial Value	Range Evaluated	History matched
K_a (mD)	3.35	2.51/4.18	3.7
S_{wi} (%)	0.273	0.270/0.275	0.273
S_{orw} (%)	0.333	0.32/0.34	0.34
K_{romax}	0.425	0.32/0.53	0.460
K_{rwmax}	0.334	0.25/0.42	0.465
N_w	2	1.5/2.5	1.8
N_o	2	1.5/2.5	1.6

results were not able to represent experimental results found in the core flooding CF-2, especially the delay in oil production, history matching was performed using the tuning parameters described in section 2.2.2 (blend adsorption and IFT). Preliminary attempts were made to adjust the oil production profile by increasing the IFT value and the surfactant adsorption. Rising the IFT value above 0.1 mN/m did not properly reproduce the delay in oil production (neither the slope of the production profile nor the total recovered oil). However, it was noticed that an increase in surfactant adsorption to very high levels (30 mg/g) better matched the simulated results with the experimental ones. At that point, it was obvious that surfactant adsorption would have a greater influence on the performance of chemical flooding than other parameters. Thus, a history matching study was carried out using the tuning parameters described previously for chemical flooding, but with special attention on the surfactant adsorption, expanding its evaluation range. The relative permeability curves for water flooding (Set 1) and completely miscible flooding (Set 2) used for curve interpolation during history matching are shown in Fig. 9.

Table 7 presents the initial values and range of evaluation used in the simulation. A total of 800 models were generated with different values and combinations of these parameters, using the established range of variations. Fig. S8 and S9 (in SI) show outcomes of the 800 models. The defined values after the history matching are also shown in Table 7. With these parameters, the model's global error was 8.21%.

Since the blend adsorption was already evaluated experimentally at 25 °C, the most likely explanation for this performance is to assume that this adsorption is actually the total retention of the surfactant in the porous medium, which involves the adsorption on the rock and also retention in the immovable oily phase contained in the pores of the rocks. The partitioning of the surfactant towards the oil phase (phase trapping) would justify the excess retention levels (Glover et al., 1979; Jang et al., 2016; Novosad, 1982). That would mean the microemulsion has shifted from Winsor type III to Winsor type II (water in oil microemulsion). Once the surfactant concentration in the oil phase is equilibrated, the oil begins to be movable. Moreover, the incorporation of water into the oil phase induces an increase in the emulsion viscosity, which would justify increases of the differential pressure along the surfactant injection (Izadi et al., 2014). The pressure behavior was therefore modeled by increasing the emulsion viscosity along the injection (Al-Murayri et al., 2019; CMG, 2016; Goudarzi et al., 2013).

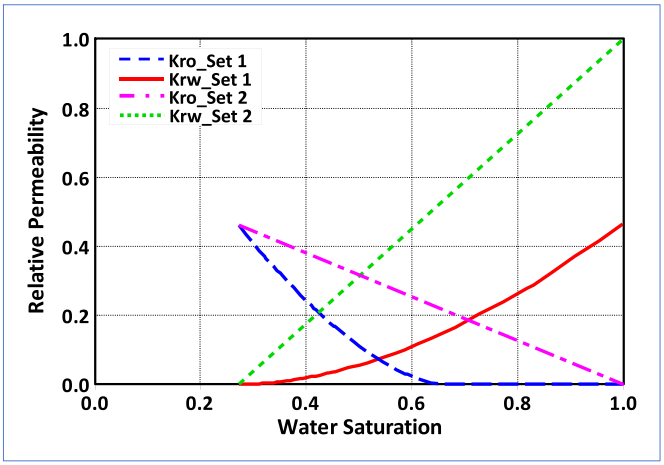

Fig. 9. Relative permeability curves for high IFT (Set 1) and ultralow IFT (Set 2), CF-2 model.

Table 7
Set of parameters for history matching of surfactant flooding, test CF-2.

Parameter	Initial value	Range evaluated	History matched
Dtrapw_Set 1	−5	−6.25/−3.75	−4.01
Dtrapn_Set 1	−5	−6.25/−3.75	−5.13
Dtrapw_Set interm	−3.5	−4.37/−2.62	−2.84
Dtrapn_Set interm	−3.5	−4.37/−2.62	−3.38
Dtrapw_Set 2	−2	−2.5/−1.5	−2.15
Dtrapn_Set 2	−2	−2.5/−1.5	−2.12
Surfactant Adsorp (mg/g)	0.60	0.60/50	36.4

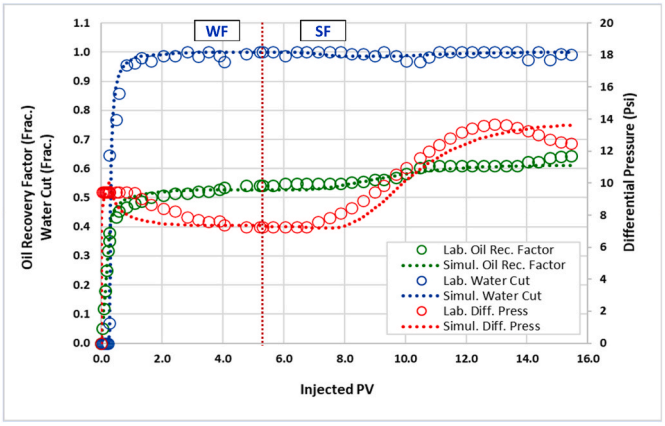

Fig. 10. Results of history matching process for core flooding test CF-2. Injection rate of 0.066 mL/min (~1 ft/D) at 120 °C.

Fig. 10 shows the results of the history matching evaluation, with experimental and best matched profiles for the objective variables.

The shift of the microemulsion behavior from Winsor type III to type II found by simulation could be due to an increase in water phase salinity or temperature. The phase behavior of the blend SDBS/C1EG was evaluated for salinity increase until 10% TDS and no shift was observed (Somoza et al., 2022b). In this work, microemulsion behavior was analyzed up to a temperature of 75 °C (see section 3.1.1), and despite showing a reduction of solubilization parameters with increasing temperature, the microemulsion always remained Winsor type III. Higher temperatures could not be tested due to working at atmospheric pressure and the corresponding boiling temperatures of the fluids. Taking into account the change of salinity from SFW to SSW inside the core during the SSW flooding, the amount of PV of SSW injected in CF-2 test, and the low effect of the salinity increase on the very similar blend SDBS/C1EG, the possible change of microemulsion type during the flooding could be very likely due to the increase of the test temperature.

- ***CF-3 test***

With regard to the CF-3 test, a simulation was done to validate the IFT and adsorption values obtained experimentally in sections 3.1.3 and 3.1.4 respectively, and later to optimize the process. The steps followed to simulate and to history match the water flooding were analogous to those described above for the CF-2 model. Initial and final values for the fitting parameters are shown in Table 8.

Table 8
Set of parameters for history matching of water flooding, test CF-3.

Parameter	Initial value	Range evaluated	History matched
K_a **(mD)**	17.69	16/20	17.7
S_{wi} **(frac.)**	0.402	0.39/0.405	0.402
S_{orw} **(frac.)**	0.343	0.33/0.35	0.345
K_{romax}	0.801	0.3/0.9	0.776
K_{rwmax}	0.353	0.3/0.9	0.383
N_w	2	1.5/3	1.8
N_o	2	1.5/3	1.9

Once the relative permeability curve Set 1 for the CF-3 water flooding was defined (see Fig. 9), a simulation was run for the blend and polymer injections, using experimental surfactant IFT and adsorption, and polymer RRF. Since a first suitable match was not obtained among the simulated and experimental objective variables at this stage, history matching was performed. Fig. 11 presents the relative permeability curves for water flooding (Set 1) and the ideal miscible flooding (Set 2), used for interpolation during history matching.

Table 9 shows initial and adjusted values of the tuning parameters, before and after history matching. The global error was found to be 7.91%. Fig. S10 to S.12 show several outcomes of the 800 generated models.

Fig. 12 shows a comparison between laboratory and simulated (with parameters shown in Table 9) data for produced oil, differential pressure and water cut profiles for core flooding test CF-3. It can be seen that in the case of the pressure profile for polymer injection, the simulation shows a certain deviation from experimental data, this is likely due to the plugging face not being appropriately modeled. However, regarding the surfactant parameters, a perfect match was found. So, the IFT and surfactant adsorption values were validated, and the model can be considered suitable to represent the oil displacement process.

3.2.2. Chemical injection optimization

Once the best matched simulation for the CF-3 test was obtained (base case), several schemes of chemical injection were designed (see Table 10) to determine the effects of the size of the slug and the injection rate over the final oil recovery, working at 25 °C. The ranges of variation were kept within realistic operational conditions.

The optimization focused on the blend injection. Polymer injection conditions of the base case were not modified for the first 4 cases, to avoid those improvements in the displacement control influencing the final oil recovery. Only the last case (Case 5) was simulated with a low residual resistance factor (RRF = 1.0) and a high viscosity (20 mPa S) for the polymer slug. Table 10 presents the EOR achieved in simulations of the different cases.

As expected, decreasing the mobility of the displacing fluid by injection of a more viscous polymer improves the volumetric sweep efficiency, reaching the highest values of recovered oil for the EOR process. For the other cases, although differences among them can be noted, a huge increase of the oil recovery with respect to the base case was not observed. Fig. 13 shows the oil recovery profiles for all the cases studied.

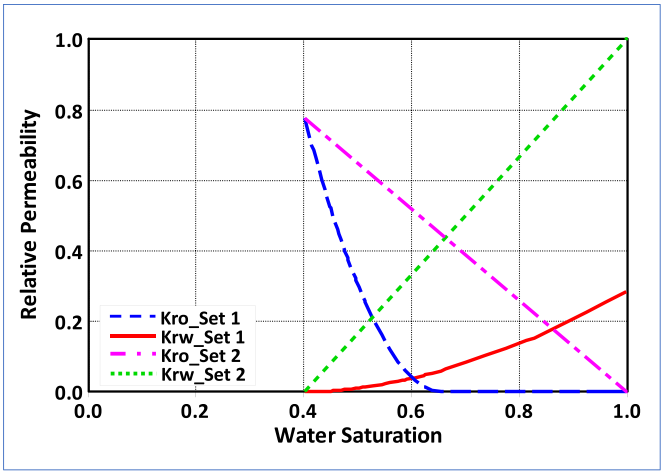

Fig. 11. Relative permeability curves for high IFT (Set 1) and ultralow IFT (Set 2), CF-3 model.

Table 9
Set of parameters for history matching of surfactant flooding, test CF-3.

Parameter	Initial value	Range evaluated	History matched
Dtrapw_Set 1	−5	−6.25/−3.75	−3.82
Dtrapn_Set 1	−5	−6.25/−3.75	−4.52
Dtrapw_Set interm	−3.5	−4.37/−2.62	−3.16
Dtrapn_Set interm	−3.5	−4.37/−2.62	−2.63
Dtrapw_Set 2	−2	−2.5/−1.5	−1.76
Dtrapn_Set 2	−2	−2.5/−1.5	−1.95
Surfactant Adsorp (mg/g)	0.60	0.45/0.75	0.63
Polymer RRF	1.4	1.05/1.75	1.69
Polymer Adsorp (mg/g)	0.50	0.37/0.62	0.38
Polymer APV	0.9	0.4/1.0	0.88

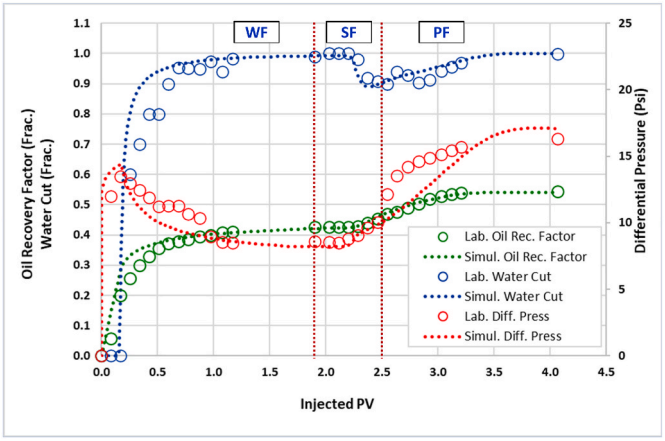

Fig. 12. Results of history matching process for core flooding test CF-3. Injection rate of 0.05 mL/min (~1 ft/D) at 25 °C.

Table 10
Case studies for the blend flooding and simulated EOR results, CF-3 test.

Case	Slug volume (PV)	Injection Rate (mL/min)	Polymer Visc. (mPa S)	AOR (% OOIP)
Base	0.56	0.05	6.3	11.5
Case 1	0.4	0.05	6.3	11.1
Case 2	1.0	0.05	6.3	12.1
Case 3	0.56	0.025	6.3	10.5
Case 4	0.56	0.075	6.3	11.7
Case 5	0.56	0.05	20	15.4

4. Conclusions

In a previous work, we proposed the use of a formulation based on the surfactant SDBS and the SAIL C1EG for EOR. The novelty of this new work lies in the approach to the industrial application of the method. To that aim, the ABS petroleum surfactant RECOLAS103 (developed by Cepsa) was blended with the SAIL, and the formulation was evaluated for EOR, both experimentally and through simulation. From the work carried out, some conclusions can be established.

The substitution of the pure commercial surfactant SDBS for the RECOLAS103 (a mixture of lineal alkyl benzene sulfonates with an average length of 11.6 carbons) did not affect any significant change regarding phase behavior, IFT and adsorption of the formulation. Blend scans showed two Winsor type III microemulsions at 25 °C, the first one around 40 wt% RECOLAS103 and the second one around 70 wt%

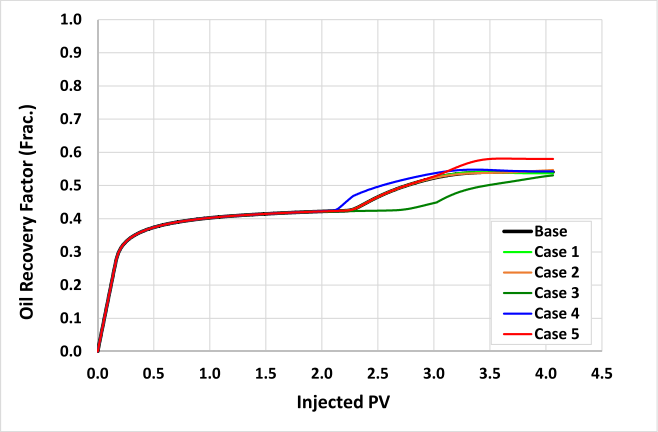

Fig. 13. Results of the optimization process for the blend injection. Injection rate of 0.05 mL/min (~1 ft/D) at 25 °C.

RECOLAS103. Based on our previous study, further evaluation was focused on the first system. The Winsor type III behavior found at 40 wt % RECOLAS103 also continued at 50 and 75 °C although the optimal solubilization parameter decreased significantly. The oil-water IFT is more affected by the type of crude oil than by the small variations in the alkyl chain length of the sulfonate surfactant.

Oil recoveries achieved at 25 and 120 °C, using different injection conditions, were higher than 10 %OOIP. High productivity was achieved at 25 °C. The combination with a polymer formulation maintains the level of recovery and can decrease the cost of the surfactant.

The numerical simulations suggest that the main cause of blend efficiency loss at reservoir conditions (120 °C) was oil trapping due to a shift of the microemulsion type from Winsor Type III to Type II, likely due to the influence of temperature. Higher oil recoveries than those obtained experimentally could be achieved if the surfactant ratio at 120 °C, to avoid the shift to a Winsor II system, and type and concentration of polymer were optimized.

Funding

Ministry of Science and Innovation and State Research Agency (AEI, 10.13039/501100011033) throughout project PGC2018-097342-B-I00, including European Regional Development Fund.

Author contributions

N. Tafur: Experimental, Simulation, Formal analysis, Writing. A. Somoza: Experimental, Review & Editing. A. Panadero: Experimental, Review & Editing. B. Rodríguez-Cabo, I. Barrio: Resources, Review & Editing. M.F. García-Mayoral: Experimental, Resources, Review & Editing. A.P. Muñuzuri: Review & Editing. A Soto: Conceptualization, Supervision, Review & Editing, Funding acquisition.

Declaration of competing interest

The authors declare that they have no known competing financial interests or personal relationships that could have appeared to influence the work reported in this paper.

Data availability

No data was used for the research described in the article.

Acknowledgements

The authors would like to thank SNF Floerger for supplying polymer

samples.

Appendix A. Supplementary data

Supplementary data to this article can be found online at https://doi.org/10.1016/j.geoen.2023.211619.

References

Abbaszadeh, M., Ren, G., 2013. Simulation techniques for surfactant phase behavior and foam flow modeling in fractured reservoirs. In: Soc. Pet. Eng. - SPE Reserv. Characterisation Simul. Conf. Exhib. RCSC 2013 New Approaches Characterisation and Modelling Complex Reserv, vol. 2, pp. 927–942. https://doi.org/10.2118/166032-ms.

Akbar, M., Alghamdi, A.H., Herron, M., Allen, D., Carnegie, A., Dutta, D., Olesen, J.-R., Chourasiya, R.D., Logan, D., Stief, D., Netherwood, R., Russell, S.D., Saxena, K., 1995. A snapshot of carbonate reservoir evaluation carbonate. Oilfield Rev. 1, 38–57.

Al-Murayri, M.T., Ghedan, S.G., Skoreyko, F., Hassan, A.A., Lara, R., Qubian, A., 2019. Compositional modeling and calibration of ASP carbonate corefloods. In: SPE Middle East Oil Gas Show Conf. MEOS, Proc.. https://doi.org/10.2118/195039-ms, 2019-March.

American Petroleum Institute- Production Department, 1990. Recommended Practices for Evaluation of Polymers Used in Enhanced Oil Recovery Operations, First. ed. American Petroleum Institute - Official Publication, Washington, DC.

Barati-Harooni, A., Najafi-Marghmaleki, A., Tatar, A., Mohammadi, A.H., 2016. Experimental and modeling studies on adsorption of a nonionic surfactant on sandstone minerals in enhanced oil recovery process with surfactant flooding. J. Mol. Liq. 220, 1022–1032. https://doi.org/10.1016/j.molliq.2016.04.090.

Bardon, C., Longeron, D.G., 1980. Influence of very low interfacial tensions on relative permeability. Soc. Petrol. Eng. J. 391–401. https://doi.org/10.2118/7609-pa.

Barnes, J.R., Smit, J.P., Smit, J.R., Shpakoff, P.G., Raney, K.H., Puerto, M.C., 2008. Development of surfactants for chemical flooding at difficult reservoir conditions. SPE Symp. Improv. Oil Recover. 1, 435–452. https://doi.org/10.2118/113313-ms.

Burchette, T.P., 2012. Carbonate rocks and petroleum reservoirs: a geological perspective from the industry. Geol. Soc. Spec. Publ. 370, 17–37. https://doi.org/10.1144/SP370.14.

CMG, 2016. In: STARS User Guide-Advanced Processes & Thermal Reservoir Simulator, Version 20. Computer Modelling Group Ltd., Calgary, Canada.

Cooper, E.R., Andrews, C.D., Wheatley, P.S., Webb, P.B., Wormald, P., Morris, R.E., 2004. Ionic liquids and eutectic mixtures as solvent and template in synthesis of zeolite analogues. Nature 430, 1012–1016. https://doi.org/10.1038/nature02860.

Feng, H., Hou, J., Ma, T., Meng, Z., Wu, H., Yang, H., Kang, W., 2018. The ultra-low interfacial tension behavior of the combined cationic/anionic-nonionic gemini surfactants system for chemical flooding. Colloids Surfaces A Physicochem. Eng. Asp. 554, 74–80. https://doi.org/10.1016/j.colsurfa.2018.06.028.

Fernández-Stefanuto, V., Corchero, R., Rodríguez-Escontrela, I., Soto, A., Tojo, E., 2018. Ionic liquids derived from proline: application as surfactants. ChemPhysChem 19, 2885–2893. https://doi.org/10.1002/cphc.201800735.

Ghadami, N., Arsanti, D., Faizal Sedaralit, M., 2015. Uncertainty assessment of chemical EOR in one of the offshore fields in Malaysia. Soc. Pet. Eng. - SPE Asia Pacific Enhanc. In: Oil Recover. Conf. EORC 2015, pp. 522–536. https://doi.org/10.2118/174614-ms.

Glover, C.J., Puerto, M.C., Maerker, J.M., Sandvik, E.L., 1979. Surfactant phase behavior and retention in porous media. Soc Pet Eng AIME J 19, 183–193. https://doi.org/10.2118/7053-pa.

Goudarzi, A., Delshad, M., Sepehrnoori, K., 2013. A critical assessment of several reservoir simulators for modeling chemical enhanced oil recovery processes. Soc. Pet. Eng. - SPE Reserv. Simul. Symp. 1, 33–48. https://doi.org/10.2118/163578-ms, 2013.

Green, D., Willhite, G.P., 2018. Enhanced Oil Recovery, second ed. Society of Petroleum Engineers, Inc, Richardson, Texas.

Hakiki, F., Maharsi, D.A., Marhaendrajana, T., 2015. Surfactant-polymer coreflood simulation and uncertainty analysis derived from laboratory study. J. Eng. Technol. Sci. 47, 706–725. https://doi.org/10.5614/j.eng.technol.sci.2015.47.6.9.

Hanke, C.G., Lynden-Bell, R.M., 2003. A simulation study of water-dialkylimidazolium ionic liquid mixtures. J. Phys. Chem. B 107, 10873–10878. https://doi.org/10.1021/jp034221d.

Harbert, L.W., 1983. Low interfacial tension relative permeability. In: Proc. - SPE Annu. Tech. Conf. Exhib, pp. 2–9. https://doi.org/10.2523/12171-ms, 1983-Octob.

Huh, C., 1979. Interfacial tensions and solubilizing ability of a microemulsion phase that coexists with oil and brine. J. Colloid Interface Sci. 71, 408–426. https://doi.org/10.1016/0021-9797(79)90249-2.

Izadi, M., Kazemi, H., Manrique, E.J., Kazempour, M., Rohilla, N., 2014. Microemulsion flow in porous media : potential impact on productivity loss. In: Soc. Pet. Eng. - SPE EOR Conf. Oil Gas West Asia, Muscat, Oman. https://doi.org/10.2118/169726-MS.

Jang, S.H., Liyanage, P.J., Tagavifar, M., Chang, L., Upamali, K.A.N., Lansakara-P, D., Weerasooriya, U., Pope, G.A., 2016. A systematic method for reducing surfactant retention to extremely low levels. SPE - DOE Improv. Oil Recover. Symp. Proc. 2016-Janua. https://doi.org/10.2118/179685-ms.

Jia, H., Leng, X., Hu, M., Song, Y., Wu, H., Lian, P., Liang, Y., Zhu, Y., Liu, J., Zhou, H., 2017. Systematic investigation of the effects of mixed cationic/anionic surfactants on the interfacial tension of a water/model oil system and their application to enhance crude oil recovery. Colloids Surfaces A Physicochem. Eng. Asp. 529, 621–627. https://doi.org/10.1016/j.colsurfa.2017.06.055.

Kamal, M.S., Hussein, I.A., Sultan, A.S., 2017. Review on surfactant flooding: phase behavior, retention, IFT, and field applications. Energy Fuel. 31, 7701–7720. https://doi.org/10.1021/acs.energyfuels.7b00353.

Kornilov, A., Zhirov, A., Petrakov, A., Rogova, T., Kurelenkova, Y., Afanasiev, I., Sansiev, G., Fedorchenko, G., Fursov, G., Kubrak, M., Altmann, T., Lichterfeld-Weber, N., Bittner, C., Oetter, G., Helwig, E., 2020. Selection of effective surfactant composition to improve oil displacement efficiency in carbonate reservoirs with high salinity formation water. In: Soc. Pet. Eng. - SPE Russ. Pet. Technol. Conf. RPTC 2019. https://doi.org/10.2118/196772-ms, 2019.

Kumar, A., Mandal, A., 2020. Core-scale modelling and numerical simulation of zwitterionic surfactant flooding: designing of chemical slug for enhanced oil recovery. J. Pet. Sci. Eng. 192 https://doi.org/10.1016/j.petrol.2020.107333.

Kurnia, I., Zhang, G., Han, X., Yu, J., 2020. Zwitterionic-anionic surfactant mixture for chemical enhanced oil recovery without alkali. Fuel 259, 116236. https://doi.org/10.1016/j.fuel.2019.116236.

Li, Y., Puerto, M., Bao, X., Zhang, W., Jin, J., Su, Z., Shen, S., Hirasaki, G., Miller, C., 2017. Synergism and performance for systems containing binary mixtures of anionic/cationic surfactants for enhanced oil recovery. J. Surfactants Deterg. 20, 21–34. https://doi.org/10.1007/s11743-016-1892-x.

Li, Z., Wu, H., Hu, Y., Chen, X., Yuan, Y., Luo, Y., Hou, J., Bai, B., Kang, W., 2020. Ultra-low interfacial tension biobased and catanionic surfactants for low permeability reservoirs. J. Mol. Liq. 309 https://doi.org/10.1016/j.molliq.2020.113099.

Ma, K., Cui, L., Dong, Y., Wang, T., Da, C., Hirasaki, G.J., Biswal, S.L., 2013. Adsorption of cationic and anionic surfactants on natural and synthetic carbonate materials. J. Colloid Interface Sci. 408, 164–172. https://doi.org/10.1016/j.jcis.2013.07.006.

Manshad, A.K., Rezaei, M., Moradi, S., Nowrouzi, I., Mohammadi, A.H., 2017. Wettability alteration and interfacial tension (IFT) reduction in enhanced oil recovery (EOR) process by ionic liquid flooding. J. Mol. Liq. 248, 153–162. https://doi.org/10.1016/j.molliq.2017.10.009.

Montes, J., Blin, N., Alvarez, A.E., Barrio, I., Panadero, A., Rodriguez, R., Coca, M., Trujillo, F., 2018. Novel anionic surfactant formulation for high temperature carbonate reservoirs. In: Soc. Pet. Eng. - SPE EOR Conf. Oil Gas West Asia. https://doi.org/10.2118/190353-ms, 2018 2018-March.

Nandwani, S.K., Chakraborty, M., Bart, H.J., Gupta, S., 2018. Synergism, phase behaviour and characterization of ionic liquid-nonionic surfactant mixture in high salinity environment of oil reservoirs. Fuel 229, 167–179. https://doi.org/10.1016/j.fuel.2018.05.021.

Nandwani, S.K., Chakraborty, M., Gupta, S., 2019. Chemical flooding with ionic liquid and nonionic surfactant mixture in artificially prepared carbonate cores: a diffusion controlled CFD simulation. J. Petrol. Sci. Eng. 173, 835–843. https://doi.org/10.1016/j.petrol.2018.10.083.

Nandwani, S.K., Malek, N.I., Chakraborty, M., Gupta, S., 2019b. Potential of a novel surfactant slug in recovering additional oil from highly saline calcite cores during the EOR process: synergistic blend of surface active ionic liquid and nonionic surfactant. Energy Fuel. 33, 541–550. https://doi.org/10.1021/acs.energyfuels.8b03419.

Novosad, J., 1982. Surfactant retention in berea sandstone-effects of phase behavior and temperature. Soc. Petrol. Eng. J. 22, 962–970. https://doi.org/10.2118/10064-PA.

Pal, N., Vajpayee, M., Mandal, A., 2019. Cationic/nonionic mixed surfactants as enhanced oil recovery fluids: influence of mixed micellization and polymer association on interfacial, rheological, and rock-wetting characteristics. Energy Fuel. 33, 6048–6059. https://doi.org/10.1021/acs.energyfuels.9b00671.

Puerto, M., Hirasaki, G.J., Miller, C.A., Barnes, J.R., 2012. Surfactant systems for EOR in high-temperature, high-salinity environments. SPE J. 17, 11–19. https://doi.org/10.2118/129675-PA.

Rodriguez-Escontrela, I., Puerto, M.C., Miller, C.A., Soto, A., 2017. Ionic liquids for low-tension oil recovery processes: phase behavior tests. J. Colloid Interface Sci. 504, 404–416. https://doi.org/10.1016/j.jcis.2017.05.102.

Ronde, H., 1992. Relative permeability at low interfacial tensions. In: Proc. - SPE Annu. Tech. Conf. Exhib. Sigma, pp. 123–134. https://doi.org/10.2523/24877-ms.

Scamehorn, J.F., Schechter, R.S., Wade, W.H., 1982. Adsorption of surfactants on mineral oxide surfaces from aqueous solutions. I: isomerically pure anionic surfactants. J. Colloid Interface Sci. 85, 463–478. https://doi.org/10.1016/0021-9797(82)90013-3.

Sharma, H., Lu, J., Weerasooriya, U.P., Pope, G.A., Mohanty, K.K., 2016. Adsorption in chemical floods with ammonia as the alkali. SPE - DOE Improv. In: Oil Recover. Symp. Proc. https://doi.org/10.2118/179682-MS, 2016-Janua.

Sheng, J., 2013. Enhanced Oil Recovery Field Case Studies, second ed. Elsevier Inc., Amsterdam.

Sheng, J., 2011. Modern Chemical Enhanced Oil Recovery: Theory and Practice, second ed. Elsevier Inc., Amsterdam.

Somoza, A., Arce, A., Soto, A., 2022a. Oil recovery tests with ionic liquids: a review and evaluation of 1-decyl-3-methylimidazolium triflate. Petrol. Sci. 19, 1877–1887. https://doi.org/10.1016/j.petsci.2021.10.025.

Somoza, A., Tafur, N., Arce, A., Soto, A., 2022b. Design and performance analysis of a formulation based on SDBS and ionic liquid for EOR in carbonate reservoirs. J. Pet. Sci. Eng. 209, 109856 https://doi.org/10.1016/j.petrol.2021.109856.

Spildo, K., Johannessen, A., Skauge, A., 2012. Low salinity waterflood at reduced capillarity. SPE - DOE Improv. Oil Recover. Symp. Proc. 2, 1264–1276. https://doi.org/10.2118/154236-ms.

Van Quy, N., Labrid, J., 1983. Numerical study of chemical flooding - comparison with experiments. Soc. Petrol. Eng. J. 23, 461–474. https://doi.org/10.2118/10202-pa.

Wang, J., Han, M., Fuseni, A.B., Cao, D., 2015. Surfactant adsorption in Surfactant-Polymer flooding for carbonate reservoirs. In: SPE Middle East Oil Gas Show Conf. MEOS, Proc, pp. 1736–1746. https://doi.org/10.2118/172700-ms, 2015-Janua.
Zabihi, S., Faraji, D., Rahnama, Y., Zeinolabedini Hezave, A., Ayatollahi, S., 2019. Relative permeability measurement in carbonate rocks, the effects of conventional surfactants vs. Ionic liquid-based surfactants. J. Dispersion Sci. Technol. 41, 1797–1811. https://doi.org/10.1080/01932691.2019.1637262.
Zhu, Y., Lei, M., 2015. Effects of crude oil components on the interfacial tension between oil and surfactant solutions. In: Soc. Pet. Eng. - SPE Asia Pacific Enhanc. Oil Recover. Conf. EORC, pp. 341–349. https://doi.org/10.2118/174593-ms, 2015.